Breaking of an Emulsion under an ac Electric Field

Abdou R. Thiam, Nicolas Bremond,* and Jérôme Bibette
UPMC Université Paris 06, CNRS UMR 7195, ESPCI ParisTech, 10 rue Vauquelin, 75231 Paris, France
(Received 3 March 2009; published 7 May 2009)

By using microfluidic chips, we investigate the stability regarding coalescence of droplet pairs under an electric field as a function of drop separation and ac field intensity. Three different regimes are found: stable, coalescence, and partial merging. From this, we identify the two breaking scenarios of a one dimensional train of droplets: in one case the coalescence front propagates; in the other case, in which pairs belong to the partial merging regime, the coalescence front can become heterogeneous. From these findings, we can propose a destruction mechanism for a macroscopic emulsion, which includes the packing condition for which total and immediate destruction is effective.

DOI: 10.1103/PhysRevLett.102.188304 PACS numbers: 82.70.Kj, 47.55.df, 83.60.Np

The coalescence of emulsion droplets induced by the presence of an ac electric field can be a beneficial phenomenon used for enhancing the destruction of water in oil emulsions, such as, for example, in oil recovery technologies [1], or more recently for controlling the fusion of individual droplets in digital microfluidic applications [2]. Following the pioneering work of Rayleigh [3] on the bursting of charged drops and experimental studies on disintegration of drops submitted to high voltage [4], Taylor [5] analyzed the stability of a drop raised to a fixed potential or floating in an external electric field. This analysis has been extended to a situation where two drops are interacting under a field and may eventually coalesce [6–8]. Here, we revisit, by using a microfluidic setup, the coalescence stability diagram of droplet pairs under an ac field, and extend this to the merging condition of a train of drops. For pairs, we show the existence of three regions: stable, coalescence, and partial merging. For trains, we identify two scenarios of breaking: in one case the coalescence front propagates, in the other case, the coalescence front becomes heterogeneous, in agreement with the pair stability diagram, which in that situation would exhibit partial merging. From these results, we can propose a destruction mechanism for a macroscopic emulsion sample and clarify the packing condition for which total and immediate destruction is effective.

As previously demonstrated [9], the use of microfluidic technology is well suited to experimental investigations on emulsion stability. Indeed, digital microfluidics allows us to control drop motion, morphology, composition and interfacial properties [10]. The microfluidic devices are made in poly(dimethylsiloxane) (PDMS) by using standard soft lithography techniques [11]. Electrodes are fabricated by filling channels with a molten solder after silanization with 3-mercaptopropyl-trimethoxysilane that ensures wettability of the solder on PDMS [12]. The channels used for casting the electrodes are patterned into the same layer of the fluidic channels. This fabrication procedure allows the generation of an electric field as homogeneous as possible along the thickness that is equal to 23 μm. As shown in Fig. 1(a), the fusion chamber, where the drop pair is aligned along the electric field direction, is sandwiched between two PDMS layers of size L_1. Assuming perfect dielectric materials and plan capacitors, the electric field within the fusion chamber is then given by $E_0 = V/(2L_1\varepsilon_c/\varepsilon_w + L_2)$, where V is the voltage difference between both electrodes, L_2 is the length of the fusion chamber, and $\varepsilon_w = 2.5$ and $\varepsilon_c = 2$ are the dielectric constant of the PDMS and the continuous phase, respectively. The electrical forcing is controlled by an arbitrary waveform generator and amplified with a high voltage amplifier (with an amplification factor of 1000). The voltage difference V imposed at the electrodes is in ac mode at a frequency of 10 kHz. The root mean square value of V is used for evaluating the electric field E_0 inside the fusion chamber.

A regular train of pairs of water in oil emulsion droplets is generated as reported in a previous study on emulsion stability [9]. The dispersed phase is either milli-Q water, with an electrical conductivity σ_d of 1.5×10^{-6} S/m, or 0.01 M and 0.1 M NaCl solutions with an electrical conductivity of around 1.2×10^{-3} S/m and 1.2×10^{-2} S/m, respectively. Hexadecane is used as the continuous oil phase in which a nonionic surfactant, Span 80, is added

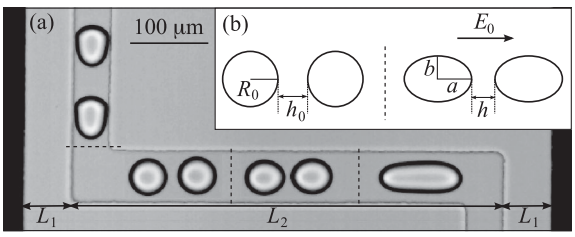

FIG. 1. (a) Microfluidic device used for the investigation of emulsion droplet coalescence under a uniform electric field. The electric field is generated by two parallel electrodes seen on both sides of the picture. The figure shows the behavior of a droplet pair that travels along the fusion chamber. (b) Sketch of two drops before and after being subjected to a uniform electric field E_0.

(1% in mass). This surfactant drops down the interfacial tension γ from 50 mN/m to 5 mN/m for the Milli-Q water and to 4 mN/m for the NaCl solutions, as measured with the ring method. The flows of both liquid phases are driven by syringe pumps. The complete history of a droplet pair, before and after being subjected to an electric field, is recorded with a high speed camera mounted on an inverted microscope. In order to avoid any electrostatic disturbances that could affect the drop pair before it enters the observation window, the voltage is applied only once every second during the traveling of the pair into the fusion chamber. Many thousands of sequences are then recorded and automatically analyzed using image processing scripts.

If an isolated and conductive solid sphere of radius R_0 floating in a dielectric medium of dielectric constant ε_c is subjected to a uniform electric field E_0, it will then distort the electric field with a maximum amplification at the poles of the drop aligned along E_0 [13]. Indeed, the sphere is polarized and generates an electric field like a dipole source. If now we consider a conductive and deformable drop, the inhomogeneity of the electrical stress σ_E induces a transition from a sphere to a prolate spheroid [5], the major axis being aligned along the field E_0 [Fig. 1(b)]. The drop can then undergo disintegration once the electrical stress $\sigma_E \sim \varepsilon_c \varepsilon_0 E_0^2$ overcomes the restoring capillary pressure $p_c \sim \gamma/R_0$, ε_0 being the vacuum permittivity. If now a second drop is in the vicinity of the first one, the electric field at the surface of the drops is amplified because of dipole-dipole interaction and becomes stronger as they come closer [14]. Therefore, the drop pair can be destabilized at lower E_0 [6,15]. For the present experimental configuration, the drops are confined and have an initial pancakelike shape. Then, the drops become squeezed prolate spheroids once the electric field is turned on.

Before investigating the collective behavior of many drops, we first focus on the interaction between two of them. In our experiments, we set the average initial gap h_0 between the drops by adding oil to the main flow after the formation of the droplet pairs [9]. The characterization of the pair behavior is conducted during a period of time for which the relative distance between the two centers of mass essentially does not change (less than 1%). Indeed, because of the neighboring drop, each of them experiences a dielectrophoretic force that drives them toward one another [16] and thus can induce a slight decrease of the separation. In addition, because of inherent fluctuations of the flow rate due to the syringe pump system, the drop size R_0 as well as the gap thickness h_0 are fluctuating. These fluctuations are a key aspect of our experiments since they allow us to scan very slight variations of initial conditions regarding R_0 and h_0. Along the several experimental runs, the ratio between the standard deviation and the mean varies from 2% to 4% for R_0 and from 20% to 70% for h_0. The stability diagram (h_0, E_0) can then be obtained.

If the ratio h_0/R_0 is sufficiently large, the drops become elongated and adopt an elliptical shape for which the ratio a/b reaches a plateau after a few hundreds of microseconds [Fig. 2(a)]. When the relative separation is slightly smaller, we observe partial merging: the drops start to coalesce and are transiently connected via a liquid bridge that ultimately breaks, after which the drops surprisingly repel [Fig. 2(b)]. For an even smaller gap thickness, the liquid bridge can grow and the two neighboring drops coalesce after less than a millisecond [Fig. 2(c)]. We note that these features are somehow similar to electrowetting experiments but where the stability of the liquid bridge is governed by the contact angle on the solid boundaries [17].

After processing the sequences recorded for various conditions as shown in Fig. 2, we can then construct the drop pair stability phase diagram. In Fig. 3, we report the final stage of the drop pairs within ($\tilde{h}_0$, $\tilde{E}_0$) phase diagrams, where $\tilde{h}_0 = h_0/R_0$ and $\tilde{E}_0 = E_0(\varepsilon_c \varepsilon_0 R_0/\gamma)^{1/2}$, for three different electric conductivities. As suggested by the observations reported in Fig. 2, we indeed identify three different regions: region 1, drops are stable; region 2, drop interfaces are unstable and drops coalesce; region 3, drop interfaces are unstable but drops do not coalesce. We first notice that the frontier separating stable and unstable pairs remains essentially the same for different conductivities. In addition, this frontier follows qualitatively the same trend as previously observed and predicted for a system made of water drops in air [6]: the critical electric field strength, beyond which the drop pair is unstable,

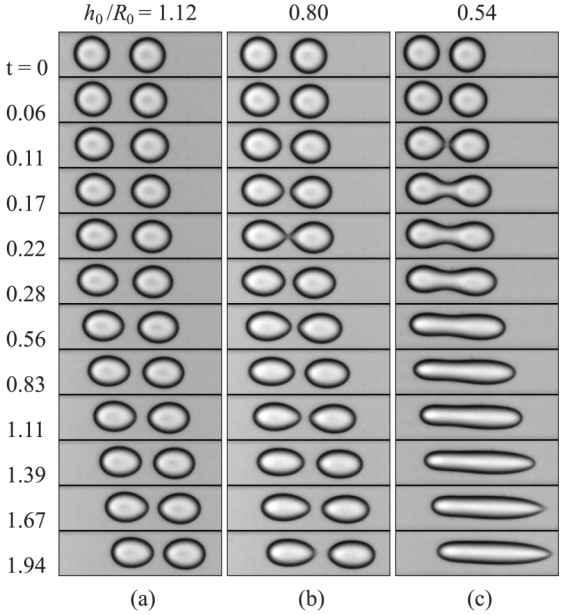

FIG. 2. Time series showing the different behaviors of a pair of water drops with a NaCl concentration of 0,01 M subjected to an ac electric field $E_0 = 2730$ kV/m at a frequency of 10 kHz. The time in millisecond is indicated on the left-hand side and the mean drop radius R_0 is around 20 μm.

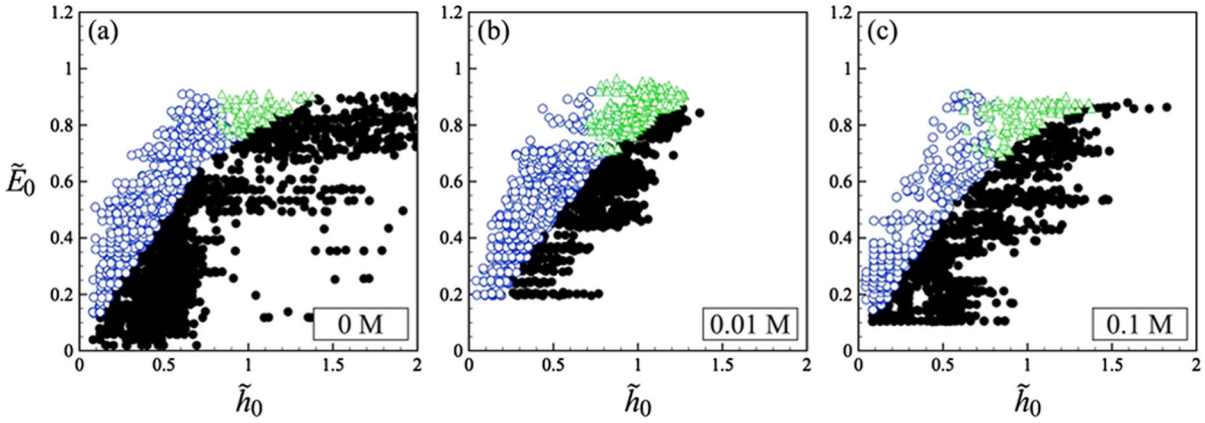

FIG. 3 (color online). Phase diagrams of two drops initially separated by $\tilde{h}_0 = h_0/R_0$ and subjected to an ac electric field $\tilde{E}_0 = E_0(\varepsilon_c \varepsilon_0 R_0/\gamma)^{1/2}$ for three electrical conductivities (the salt concentration in molar is noted on each plot). Three regions corresponding to different final states of the pair of drops are distinguished: region 1, drops are stable (●); region 2, drop interfaces are unstable and drops coalesce (○); region 3: drop interfaces are unstable but drops do not coalesce (△).

decreases when the drops get closer due to the enhancement of the electric field at the two facing poles [14].

For region 3, the interface instability can lead to two different behaviors depending on electric conductivity. For intermediate and high conductivities, the liquid bridge becomes intermittent (or eventually switches to jetting), as shown in Fig. 2(b). By contrast, for ultra low conductivity, we observe almost stable thin bridges. Indeed, in that situation, the liquid bridge that connects the two drops is stable though drops are moving away from each other as shown in Fig. 4. It is known that a longitudinal electric field helps to stabilize a liquid cylinder against the Plateau-Rayleigh breakup [18,19]. However, it is generally assumed that the characteristic time related to the charge relaxation $\tau_r = \varepsilon_d/\sigma_d$ is infinitely small. Therefore, the equilibrium state, where charges reside on the interface, is supposed to be reached instantaneously. In our experiments, the stabilization of a thin liquid bridge occurs when the forcing period $T = 100$ μs is of the order of $\tau_r = 120$ μs for milli-Q water. The origin of this stabilization may be similar to the one attributed to the observation of sharp ac cones in electrospraying experiments [20]. The authors suggest that a net charge at the interface is built up that stabilizes the cone due to mutual Coulombic repulsion between the free charges [19,20].

From these phase diagrams, we can therefore define a critical gap thickness $\tilde{h}_0^*$ given by the intersection of the three regions beyond which coalescence is inhibited. We note that this critical gap thickness slightly decreases as the electric conductivity σ_d of the water drops increases.

We now consider the behavior of a train of drops for which the field strength and the drop separation can be controlled. The microfluidic chip is such that the electric field is aligned along the drop centers. Figure 5 shows the destabilization of a train of drops subjected to an ac field for two different electric conductivities σ_d. For a high σ_d, the behavior of the train of drops can be deduced from the previous diagram shown in Fig. 3(c). Indeed, all of the pairs that have a drop-drop separation lower than $\tilde{h}_0^*$ coalesce. While drop pairs (eventually made out of merged drops), which have an initial gap thickness higher than $\tilde{h}_0^*$, do not coalesce. Once two drops merge, the field increases at the two facing poles of neighboring drops [14]; however, it does not lead to coalescence. This in agreement with the previous diagram for pairs. The behavior observed in Fig. 5(b), which corresponds to an ultra low conductivity, is different. Indeed, we observe the propagation and the acceleration of a coalescence front. In addition, this scenario occurs for a droplet separation which is set at a value larger than $\tilde{h}_0^*$. Thus the collection of drops behaves differently as compared to pairs for the same initial conditions. To observe this propagation, we must trigger the first coalescence event. To do so, a deformation is imposed at one extremity of the train while the drops flow through the converging end of the fusion chamber. The mechanical energy that deforms the drop contributes to the jump of the drop pair from a stable state to an unstable state [7]. As

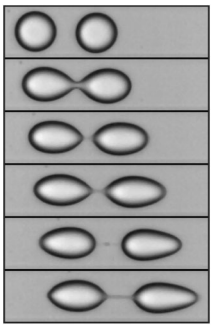

FIG. 4. Formation of a thin liquid bridge between two milli-Q water drops with an initial relative gap thickness $h_0/R_0 = 1$. The average drop radius is around 20 μm and the time step between two frames is 0.17 ms.

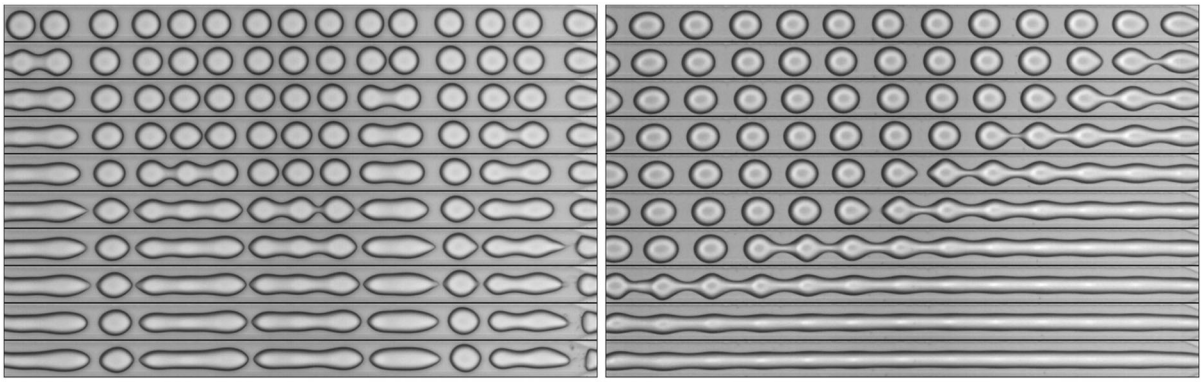

FIG. 5. Time sequences showing the propagation or not of a coalescence front among a chain of water-in-oil drops, (a) 0, 1 M NaCl solution, (b) milli-Q water. The electric field is aligned along the train of drops which have an average radius of 21 μm. The time step is 0.13 ms.

previously discussed, once the first drop pair coalesce, the resulting drop size becomes larger and the electric field between the next neighboring drop increases [14]. However, by contrast with the pair phase diagram shown in Fig. 3(a), full coalescence occurs. Indeed, within a train, the drops cannot move away from each other. Thus, the liquid bridge can expand laterally instead of being stretched. That is what is responsible for the coalescence propagation.

In this Letter, we have characterized the stability of drop pairs under an electric field as a function of drop separation. We have shown the existence of a critical relative separation above which coalescence is inhibited, independently of the ac field value. This criterion holds for droplet trains, but fails for ultra low dispersed phase conductivity. In that case, a coalescence front propagates once it is nucleated. We believe these results rationalize the pathway through which phase separation of a dense emulsion under an ac field can occur. Indeed, because the relative drop separation is linked to the drop concentration in a dense three-dimensional system, a critical volume fraction beyond which instantaneous phase separation is inhibited must be hypothesized. However, as long as the drop conductivity remains sufficiently low, a full propagative destruction must be observed.

We acknowledge Laurent Boitard and Enric Santanach for their help during electrodes fabrication. This work was supported by the European Network MiFem under Contract No. 028417 and the ANR under Grant No. 05 BLAN 039704.

*Nicolas.Bremond@espci.fr

[1] J. S. Eow, M. Ghadiri, A. O. Sharif, and T. J. Williams, Chem. Eng. J. (London) **84**, 173 (2001).
[2] K. Ahn, J. Agresti, H. Chong, M. Marquez, and D. A. Weitz, Appl. Phys. Lett. **88**, 264105 (2006).
[3] L. Rayleigh, Proc. London Math. Soc. **s1-14**, 170 (1882).
[4] J. Zeleny, Phys. Rev. **10**, 1 (1917).
[5] G. I. Taylor, Proc. R. Soc. A **280**, 383 (1964).
[6] J. Latham and I. W. Roxburgh, Proc. R. Soc. A **295**, 84 (1966).
[7] R. S. Allan and S. G. Mason, J. Colloid Sci. **17**, 383 (1962).
[8] M. Chabert, K. D. Dorfman, and J. L. Viovy, Electrophoresis **26**, 3706 (2005).
[9] N. Bremond, A. R. Thiam, and J. Bibette, Phys. Rev. Lett. **100**, 024501 (2008).
[10] A. Huebner, S. Sharma, M. Srisa-Art, F. Hollfelder, J. B. Edel, and A. J. Demello, Lab Chip **8**, 1244 (2008).
[11] J. C. McDonald, D. C. Duffy, J. R. Anderson, D. T. Chiu, H. K. Wu, O. J. A. Schueller, and G. M. Whitesides, Electrophoresis **21**, 27 (2000).
[12] A. C. Siegel, S. S. Shevkoplyas, D. B. Weibel, D. A. Bruzewicz, A. W. Martinez, and G. M. Whitesides, Angew. Chem., Int. Ed. **45**, 6877 (2006).
[13] L. Landau and E. Lifchitz, *Physique Théorique, Tome 8: Electrodynamique Des Milieux Continus* (Mir, Moscow, 1990).
[14] M. H. Davis, Q. J. Mech. Appl. Math. **17**, 499 (1964).
[15] G. I. Taylor, Proc. R. Soc. A **306**, 423 (1968).
[16] J. C. Baygents, N. J. Rivette, and H. A. Stone, J. Fluid Mech. **368**, 359 (1998).
[17] A. Klingner, J. Buehrle, and F. Mugele, Langmuir **20**, 6770 (2004); J.-C. Baret, M. M. J. Decre, and F. Mugele, Langmuir **23**, 5173 (2007).
[18] D. A. Saville, Phys. Fluids **13**, 2987 (1970).
[19] M. M. Hohman, M. Shin, G. Rutledge, and M. P. Brenner, Phys. Fluids **13**, 2201 (2001).
[20] N. Chetwani, S. Maheshwari, and H.-C. Chang, Phys. Rev. Lett. **101**, 204501 (2008).